The role of the ionic radius in the ethylene polymerization catalyzed by new group 3 and lanthanide scorpionate complexes

Gino Paolucci [a,*], Marco Bortoluzzi [a], Mariagrazia Napoli [b],
Pasquale Longo [b,**], Valerio Bertolasi [c]

[a] Dipartimento di Chimica, Università Ca' Foscari di Venezia, Dorsoduro 2137, 30123 Venezia, Italy
[b] Dipartimento di Chimica, Università di Salerno, Via Ponte don Melillo, 84084 Fisciano, SA, Italy
[c] Dipartimento di Chimica e Centro di Strutturistica Diffrattometica, Università di Ferrara, via Borsari 46, 44100 Ferrara, Italy

A R T I C L E   I N F O

A B S T R A C T

A series of new monomeric group 3 and lanthanide [N,N,N]-heteroscorpionate triflate-complexes [Ln(OTf)$_2$(cybpamd)(THF)] {Ln = Sc (**2**), Y (**3**), La (**4**), Nd (**5**), Sm (**6**), Dy (**7**), Yb (**8**); OTf = SO$_3$CF$_3$; cybpamd = N,N'-dicyclohexyl-2,2-bis-(3,5-dimethyl-pyrazol-1-yl)-acetamidinate} has been synthesized and characterized. The behavior of **2**–**8** as catalysts in olefin polymerization was investigated after proper activation with methylaluminoxane and the comparative results are reported. The activity of the catalytic systems towards ethylene polymerization is affected by the nature of the metal center and linearly grows with the ionic radius, with the exception of the scandium derivative. From DFT calculations it was possible to correlate the activity data with computed properties of the metal–alkyl bonds of the catalytically active species. The very narrow polydispersivities showed that all the considered systems act as single-site catalysts and high-weight linear polyethylene polymers were always obtained.

© 2009 Elsevier B.V. All rights reserved.

1. Introduction

In addition to the first examples of scandium, yttrium, lanthanum and f-block metals homoleptic hydrotris(pyrazolyl)borate complexes, MTp$_3$ [1], homo- and heteroscorpionate ligands have shown to be very interesting species for the synthesis of a wide range of stable group 3 elements and lanthanide derivatives [2]. As a result of the variable size of the Ln(III) ions, the predominant ionic bonding and the well-known oxofilicity of these metals, the usual coordinative unsaturation of their complexes, the presence of hard donor atoms and the ligand charge are critical factors in controlling the coordination number, the geometry and the architecture of their complexes and the isolation of well-defined molecular species. Scorpionates represent an attractive and versatile choice, due to the fine-tuning of the electronic and steric properties of these ligands and consequently the control of the metal coordination sphere.

Polyolefins can be obtained in the presence of several neutral and cationic alkyl complexes of the rare-earth metals, stabilized by both cyclopentadienyl- and non-cyclopentadienyl ancillary ligands [3] and the expected electrophilicity of group 3 metals makes them attractive as homogeneous catalysts for Ziegler-Natta polymerization. From a catalytic point of view the preparation of new scorpionate derivatives of early-d and f-block elements is a currently active field of research, as this type of complexes showed to be, among all, potentially interesting non-cyclopentadienyl Ziegler-Natta homogeneous catalysts in olefin polymerization, as observed for Sc, Y and lanthanides derivatives with substituted tris(pyrazolyl)methane and tris(pyrazolyl)borate ligands [4].

Our recent research interest in the fields of organometallic chemistry and olefin polymerization has been mainly devoted to group 3 and lanthanide-based catalysts with polydentate ligands containing nitrogen-donor groups [5]. We have currently extended our studies to heteroscorpionate bis-pyrazol-1-yl-acetamidinate anionic ligands, whose lithium, magnesium and zinc derivatives have recently shown to be active initiators for the ring-opening polymerization of cyclic esters [6].

In the last few years group 3 metal triflates have been received great attention for their ability to promote a wide variety of organic reactions [7]. In this paper we report the synthesis of a series of new neutral group 3 and lanthanide triflate-complexes with the [N,N,N]-scorpionate ligand N,N'-dicyclohexyl-2,2-bis-(3,5-dimethyl-pyrazol-1-yl)-acetamidinate (cybpamd), together with the comparison of their catalytic behavior towards ethylene polymerization.

* Corresponding author. Tel.: +39 0412348563; fax: +39 0412348684.
** Corresponding author. Tel.: +39 089969564; fax: +39 089969603.
E-mail address: paolucci@unive.it (G. Paolucci).

2. Experimental

2.1. Materials and methods

All inorganic manipulations were carried out under oxygen- and moisture-free atmosphere in a Braun MB 200 glove-box with a purifying unity G-II and equipped with apparatus for high and low temperature reactions. All the solvents were thoroughly deoxygenated and dehydrated under argon by refluxing over suitable drying agents, while NMR deuterated solvents (Euriso-Top products) were kept in the dark over molecular sieves. The anhydrous triflate salts $Ln(OTf)_3$ {Ln = Sc, Y, La, Nd, Sm, Dy, Yb; $OTf = SO_3CF_3$} and YCl_3 (Strem, Aldrich) and the organic compounds 3,5-dimethylpyrazole and N,N′-dicyclohexylcarbodiimide (Aldrich) were used as received. Butyllithium (1.6 M solution in hexanes) was purchased from Aldrich. Bis(3,5-dimethyl-pyrazol-1-yl)methane was synthesized from 3,5-dimethylpyrazole and dichloromethane on the basis of a reported procedure [8] and purified by crystallization from hot cyclohexane solutions.

All the polymerization operations were carried out under nitrogen atmosphere by using conventional Schlenk-line techniques. Methylaluminoxane (10% in toluene, Witco) was used as a solid after distillation of solvent. Ethylene (>98%), was purchased from Aldrich.

2.2. Characterizations

Microanalyses (C, H, N, Cl) of ligands and complexes were made at the Istituto di Chimica Inorganica e delle Superfici, CNR, Padova. ^1H NMR, homodecoupled ^1H NMR, ^1H COSY, ^1H NOESY, ^{13}C {^1H} NMR, ^{13}C APT, HSQC and HMBC spectra were recorded at 298 K on a Bruker Avance 300 spectrometer operating at 300 MHz (^1H) and 75 MHz (^{13}C) and referred to internal tetramethylsilane. The SwaN-MR and MestRe-C software packages were used for NMR spectroscopic data treatment [9]. Mass spectra (E.I., 70 eV) of lanthanum derivative and of the paramagnetic compounds were recorded on a Finnigan Trace GC–MS equipped with a probe controller for the sample direct inlet. The assignments were done by comparison between theoretical and experimental isotopic clusters and the most intense signals of each characterized cluster are reported.

Semi-empirical computational geometry optimizations were carried out with the MOPAC2007 software package [10]. In all the calculations the PM6 Hamiltonian [11] was used and the paramagnetic lanthanides ions were simulated using the sparkle model [12]. Calculations were carried out without symmetry constrains. Scandium, yttrium and lanthanum derivatives were also optimized with the restricted EDF1 DFT functional [13] in combination with the ECP-based LACVP* basis set [14]. Charges derived from Mulliken population analysis [15]. The software used was Spartan '08 [16]. All the calculations were carried out on a Intel Core I7-based x86-64 computer.

The samples of polyethylene for ^{13}C NMR analysis were prepared by dissolving polymer sample (40 mg) into tetrachloro-dideutero-ethane (0.5 mL). The spectra were recorded at 100 °C using hexamethyldisiloxane (HMDS) as internal chemical shift reference. The Gel Permeation Chromatography (GPC) analysis of the samples were carried out at 135 °C by Waters instrument GPCV 2000 equipped with refractive index and viscosimeter detectors, using four PSS columns set consisting of, 105, 104, 103, 102 Å (pore size) – 10 μm (particle size). o-Dichlorobenzene was the carrier solvent used with a flow rate of 1.0 mL/min. The calibration curve was established with polystyrene standards. Differential Scanning Calorimetry analysis have been carried out on a DSC 2920 apparatus manufactured by TA Instruments, calibrated against an indium standard (Tm = 156.6 °C), with heating scans from −10 to 200 °C, at a 10 °C/min heating rate, under a flowing nitrogen atmosphere. Specimens were sealed in aluminum pans.

2.3. Synthesis of N,N′-dicyclohexyl-2,2-bis-(3,5-dimethyl-pyrazol-1-yl)-acetamidine (cybpamd-H) ($C_{24}H_{38}N_6$, $M_W = 410.60$)

A solution of bis(3,5-dimethyl-pyrazol-1-yl)methane (2.000 g, 9.8 mmol) in anhydrous THF (50 mL) was cooled to −70 °C, then a 1.6 M solution in hexanes of butyllithium (6.1 mL) was added dropwise during about half an hour by maintaining the temperature as constant as possible. The resulting solution was allowed to slowly reach −10 °C and then maintained at this temperature for 20 min. The reaction mixture was cooled again at −70 °C and a solution of N,N′-dicyclohexylcarbodiimide (2.02 g, 9.8 mmol) in 20 mL of THF was slowly added. Once the addition was ended, the system was allowed to reach room temperature and left 4 h under stirring. Cold water (30 mL) was added to quench the reaction and THF was quite completely removed by evaporation under reduced pressure. The crude product was extracted with diethylether (3× 50 mL) and the resulting organic fraction was dried over $MgSO_4$. The solvent was then removed under reduced pressure and the residual oil was purified by chromatography on silica gel, using a 1:1 mixture of hexane–ethyl acetate as eluent. After in vacuo removal of the solvents the residue was dissolved in pentane (20 mL) and the resulting solution was passed on filter paper to remove eventual traces of unreacted bis(3,5-dimethyl-pyrazol-1-yl)methane. Pentane was finally removed by evaporation under reduced pressure and the product was collected as white microcrystals. Yield = 3.550 g, 88%.

Elemental analysis: found (%): C 69.9, H 9.30, N 20.4. Calcd. for $C_{34}H_{38}N_6$ (%): C 70.20, H 9.33, N 20.47.

2.4. Synthesis of [YCl₃(cybpamd-H)] (1) ($C_{24}H_{38}Cl_3N_6Y$, $M_W = 685.86$)

A solution of cybpamd-H (0.410 g, 1.0 mmol) in THF (15 mL) was added at room temperature to a suspension of anhydrous YCl_3 (1.0 mmol, 0.195 g) in 15 mL of THF. The resulting reaction mixture was allowed to react overnight at room temperature, then the solvent was removed by in vacuo evaporation and dichloromethane (30 mL) was added. The CH_2Cl_2 solution was centrifuged and subsequently concentrated to ca. 10 mL under reduced pressure. Hexane was slowly added until the product separated as solid, which was collected by filtration after about 1 h under stirring, washed with n-hexane and dried in vacuo. Yield = 0.522 g, 86%.

Elemental analysis: found (%): C 47.4, H 6.30, N 13.8, Cl 17.5. Calcd. for $C_{24}H_{38}N_6$ (%): C 47.58, H 6.32, N 13.87, Cl 17.55.

2.5. Synthesis of [Ln(OTf)₂(cybpamd)(THF)] {Ln = Sc, $C_{30}H_{45}F_6N_6O_7S_2Sc$, $M_W = 824.79$ (2); Ln = Y, $C_{30}H_{45}F_6N_6O_7S_2Y$, $M_W = 868.74$ (3); Ln = La, $C_{30}H_{45}F_6LaN_6O_7S_2$, $M_W = 918.74$ (4); Ln = Nd, $C_{30}H_{45}F_6N_6NdO_7S_2$, $M_W = 924.08$ (5); Ln = Sm, $C_{30}H_{45}F_6N_6O_7S_2Sm$, $M_W = 930.20$ (6); Ln = Dy, $C_{30}H_{45}F_6N_6O_7S_2Dy$, $M_W = 942.34$ (7); Ln = Yb, $C_{30}H_{45}F_6N_6O_7S_2Yb$, $M_W = 952.88$ (8); $OTf = SO_3CF_3$}

The same synthetic approach was applied for the preparation of all the 2–8 complexes. In a typical synthesis a solution of cybpamd-H (0.410 g, 1.0 mmol) in THF (15 mL) was added at room temperature to a THF solution (15 mL) containing 1.0 mmol of the proper anhydrous triflate salt $Ln(OTf)_3$ {Ln = Sc, Y, La, Nd, Sm, Dy, Yb}. After 20 min 12.5 mL of a 0.08 M solution of butyllithium in hexane and THF, prepared by diluting with THF the commercial solution, was added dropwise in about 15 min. The resulting mixture was allowed to react at room temperature for 12 h, then the

solvent was removed by *in vacuo* evaporation and dichloromethane (30 mL) was added to the residue. The CH_2Cl_2 solution was centrifuged to remove the solids and then concentrated to ca. 5 mL under reduced pressure. n-Hexane was slowly added until the crude product started to separate as solid, which was collected by filtration after about 1 h under stirring. The product was purified by dissolving the crude solid in 50 mL of a 20:1 diethylether–THF solution. The resulting solution was filtered and then concentrated to about 10 mL under reduced pressure. By slow addition of hexane the product separated out as microcrystals, which were filtered, washed with hexane and dried *in vacuo*. Yields: (**2**) 0.558 g, 68%; (**3**) 0.621, 71%; (**4**) 0.644 g, 70%; (**5**) 0.605 g, 65%; (**6**) 0.613 g, 65%; (**7**) 0.615 g, 65%; (**8**) 0.701 g, 74%.

Elemental analysis for **2**: found (%): C 43.5, H 5.45, N 10.15. Calcd. for $C_{30}H_{45}F_6N_6O_7S_2Sc$ (%): C 43.69, H 5.50, N 10.19. Elemental analysis for **3**: found (%): C 41.3, H 5.20, N 9.60. Calcd. for $C_{30}H_{45}F_6N_6O_7S_2Y$ (%): C 41.48, H 5.22, N 9.67. Elemental analysis for **4**: found (%): C 39.1, H 4.90, N 9.05. Calcd. for $C_{30}H_{45}F_6LaN_6O_7S_2$ (%): C 39.22, H 4.94, N 9.15. Elemental analysis for **5**: found (%): C 38.8, H 4.85, N 9.00. Calcd. for $C_{30}H_{45}F_6N_6NdO_7S_2$ (%): C 38.99, H 4.91, N 9.09. Elemental analysis for **6**: found (%): C 38.6, H 4.80, N 8.95. Calcd. for $C_{30}H_{45}F_6N_6O_7S_2Sm$ (%): C 38.74, H 4.88, N 9.03. Elemental analysis for **7**: found (%): C 38.1, H 4.85, N 8.90. Calcd. for $C_{30}H_{45}DyF_6N_6O_7S_2$ (%): C 38.24, H 4.81, N 8.92.

Characterization data for **8**. Elemental analysis: found (%): C 37.7, H 4.75, N 8.80. Calcd. for $C_{30}H_{45}F_6N_6O_7S_2Yb$ (%): C 37.81, H 4.76, N 8.82.

2.6. Polymerization runs

Polymerizations of ethylene were performed in a 250 mL glass-autoclave introducing the amount of catalyst and cocatalyst dissolved in 150 mL of toluene. The mixture was fed with the monomer and kept under magnetic stirring over the runs. The autoclave was vented and the polymerization mixture was poured in acidified ethanol. The polymers were recovered by filtration, washed with fresh ethanol and dried *in vacuo* at 60 °C.

Polymerizations of propylene were performed in a 250 mL glass-autoclave introducing 1×10^{-5} mol of catalyst (**4** or **2**) and 8.6×10^{-3} mol of MAO (based on Al) dissolved in 150 mL of toluene. The polymerization mixture was fed with propene (5 bar) and kept under magnetic stirring for 20 h. The autoclave was vented and the polymer was recovered as described for polyethylene. The polymer yield was 30 mg using catalyst **4**, while only traces of polymer were obtained using catalyst **2**.

3. Results and discussion

3.1. Synthesis and characterization of N,N′-dicyclohexyl-2,2-bis-(3,5-dimethyl-pyrazol-1-yl)-acetamidine (cybpamd-H), [YCl₃(cybpamd-H)] (**1**) and [Ln(OTf)₂(cybpamd)(THF)] complexes {Ln = Sc (**2**), Y (**3**), La (**4**), Nd (**5**), Sm (**6**), Dy (**7**), Yb (**8**); OTf = SO₃CF₃}

The organic compound *N,N′*-dicyclohexyl-2,2-bis-(3,5-dimethyl-pyrazol-1-yl)-acetamidine (cybpamd-H) has been prepared according to Otero et al. [17], i.e. by reacting bis(3,5-dimethyl-pyrazol-1-yl)methane with butyllithium in THF at low temperature to form *in situ* the corresponding lithium salt, which was subsequently reacted with one equivalent of dicyclohexylcarbodiimide. The quench of the reaction mixture with cold water allowed the formation of the final product, which was purified following common procedures and isolated in high yield (see Scheme 1). Elemental analysis (C, H, N) agreed with the proposed formulation. ¹H COSY and NOESY experiments allowed the assign-
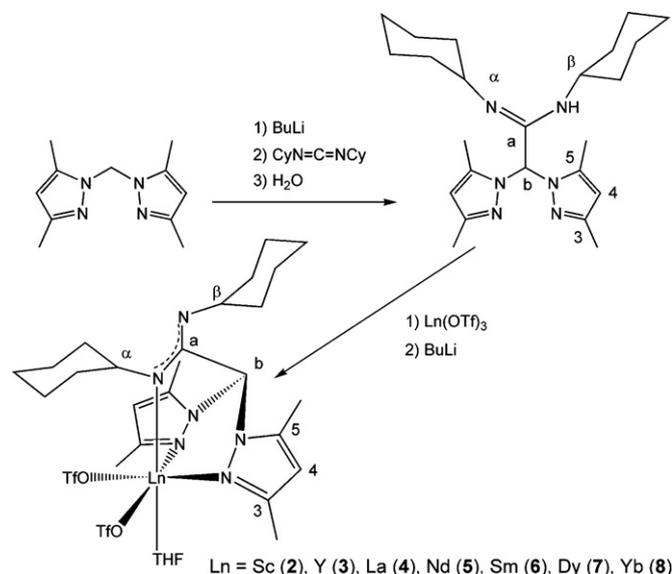
Scheme 1. cybpamd-H and [Ln(OTf)₂(cybpamd)(THF)] **2–8** syntheses and numbering.

ment of all the proton resonances of the ¹H NMR spectrum, with the exception of the –CH₂– fragments of the cyclohexyl groups far from the nitrogen atoms. The ¹³C APT (attached-proton-test), HSQC and HMBC spectra allowed to separate primary and quaternary aromatic carbons and to assign the carbon resonances. NMR data are reported in Table 1.

The neutral triflate-complexes [Ln(OTf)₂(cybpamd)(THF)] {Ln = Sc (**2**), Y (**3**), La (**4**), Nd (**5**), Sm (**6**), Dy (**7**), Yb (**8**); OTf = SO₃CF₃} were all prepared in ca. 70% yield by allowing to react cybpamd-H with a stoichiometric amount of anhydrous Ln(OTf)₃ salt in THF and subsequent addition of diluted butyllithium (see Scheme 1). The direct synthesis of these products from the lithium salt of the ligand Li[cybpamd] led always to the formation of mixtures of hardly separable products and a global lowering of the yields.

The use of stoichiometric amounts of bases such as potassium *tert*-butoxide, less strong than butyllithium, did not lead to the complete deprotonation of the coordinated ligand. Moreover, preliminary studies on the reactivity of cybpamd-H with group 3 chlorides allowed to isolate and characterize by NMR spectroscopy the complex YCl₃(cybpamd-H) (**1**). The ¹H NMR and ¹³C{¹H} NMR spectra of the yttrium complex (**1**) display the same patterns of those of cybpamd-H, with moderate variations of the chemical shift values. In the ¹H NMR spectrum of **1** the NH signal falls at 5.09 ppm, a chemical shift which is very near to the resonance of the free ligand NH proton (5.21 ppm). These data suggest that the coordination of cybpamd-H on the Ln(III) metal ions, fundamental to increase the selectivity towards the formation of the [Ln(OTf)₂(cybpamd)(THF)] derivatives, does not however strongly improve the acidity of the ligand N-bonded hydrogen atom. NMR data for compound **1** are reported in Table 1.

Elemental analyses (C, H, N) of **2–8** complexes agree with the proposed formulations. The diamagnetic compounds **2–4** have been characterized by NMR spectroscopy. The ¹H NMR spectra show downfield the signals due to the acetamidinate proton and the pyrazole-H₄. The cyclohexyl hydrogen atoms of the N-bonded CH groups fall in the range 4.0–3.0 ppm. Upfield, two sharp resonances due to the pyrazole methyl groups and the complex multiplet of the cyclohexyl methylene groups are observable. Two multiplets around 3.7 and 1.8 ppm indicate the presence of a THF molecule. The ¹³C{¹H} NMR spectra show in the range 160–140 ppm the signals due to the acetamidinate-Cₐ, the pyrazole-C₃ and pyrazole-C₅.

Table 1
Characterization data. Refer to Scheme 1 for NMR numbering.

cybpamd-H	^{1}H NMR (CDCl$_3$, 298 K): 7.14 (s, 1H) *acetamidine-H$_b$*; 5.77 (s, 2H) *pyrazole-H$_4$*; 5.21 (d, 1H, $^3J_{HH}$ = 6.7 Hz) *NH*; 3.69 (m, 1H) *cyclohexyl-NCH$_\alpha$*; 3.09 (m, 1H) *cyclohexyl-NCH$_\beta$*; 2.38 (s, 6H) *pyrazole-Me$_5$*; 2.16 (s, 6H) *pyrazole-Me$_3$*; 2.04–1.00 (m, 20H) *cyclohexyl-CH$_2$* ^{13}C{^{1}H NMR} (CDCl$_3$, 298 K): 149.2 *pyrazole-C$_3$*; 146.4 *acetamidine-C$_a$*; 141.2 *pyrazole-C$_5$*; 106.6 *pyrazole-C$_4$*; 67.5 *acetamidine-C$_b$*; 56.3 *cyclohexyl-NCH$_\beta$*; 48.0 *cyclohexyl-NCH$_\alpha$*; 35.0, 31.8, 26.0, 25.8, 24.8, 24.1 *cyclohexyl-CH$_2$*; 13.6 *pyrazole-Me$_3$*; 11.6 *pyrazole-Me$_5$*
1	^{1}H NMR (CD$_2$Cl$_2$, 298 K): 6.99 (s, 1H) *acetamidine-H$_b$*; 6.05 (s, 2H) *pyrazole-H$_4$*; 5.09 (d, 1H, $^3J_{HH}$ = 9.0 Hz) *NH*; 3.89 (m, 1H) *cyclohexyl-NCH$_\alpha$*; 3.58 (m, 1H) *cyclohexyl-NCH$_\beta$*; 2.61 (s, 6H) *pyrazole-Me$_5$*; 2.47 (s, 6H) *pyrazole-Me$_3$*; 2.08–1.05 (m, 20H) *cyclohexyl-CH$_2$* ^{13}C{^{1}H NMR} (CD$_2$Cl$_2$, 298 K): 155.4 *pyrazole-C$_3$*; 154.9 *acetamidine-C$_a$*; 141.5 *pyrazole-C$_5$*; 109.0 *pyrazole-C$_4$*; 60.5 *acetamidine-C$_b$*; 58.4 *cyclohexyl-NCH$_\beta$*; 54.8 *cyclohexyl-NCH$_\alpha$*; 35.3-24.9 *cyclohexyl-CH$_2$*; 15.0 *pyrazole-Me$_3$*; 11.8 *pyrazole-Me$_5$*
2	^{1}H NMR (CD$_3$CN, 298 K): 7.18 (s, 1H) *acetamidine-H$_b$*; 6.02 (s, 2H) *pyrazole-H$_4$*; 3.78 (m, 1H) *cyclohexyl-NCH$_\alpha$*; 3.69 (m, br, 4H) *THF*; 3.43 (m, 1H) *cyclohexyl-NCH$_\beta$*; 2.38 (s, 6H) *pyrazole-Me$_5$*; 2.16 (s, 6H) *pyrazole-Me$_3$*; 1.84 (m, br, 4H) *THF*; 1.78–1.02 (m, 20 H) *cyclohexyl* ^{13}C {^{1}H NMR} (CD$_3$CN, 298 K): 157.3 *acetamidinate-C$_a$*; 152.1 *pyrazole-C$_3$*; 143.2 *pyrazole-C$_5$*; 108.8 *pyrazole-C$_4$*; 68.4 *THF*; 65.6 *acetamidinate-C$_b$*; 56.4 *cyclohexyl-NCH$_\beta$*; 51.7 *cyclohexyl-NCH$_\alpha$*; 32.9 *cyclohexyl*; 30.8 *cyclohexyl*; 26.1 *THF*; 25.6 *cyclohexyl*; 25.5 *cyclohexyl*; 25.4 *cyclohexyl*; 23.9 *cyclohexyl*; 13.5 *pyrazole-Me$_3$*; 11.3 *pyrazole-Me$_5$*
3	^{1}H NMR (CD$_3$CN, 298 K): 6.88 (s, 1H) *acetamidine-H$_b$*; 5.96 (s, 2H) *pyrazole-H$_4$*; 3.70 (m, 4H) *THF*; 3.43 (m, 1H) *cyclohexyl-NCH$_\alpha$*; 3.21 (m, 1H) *cyclohexyl-NCH$_\beta$*; 2.41 (s, 6H) *pyrazole-Me$_5$*; 2.22 (s, 6H) *pyrazole-Me$_3$*; 1.83 (m, 4H) *THF*; 1.80–1.09 (m, 20 H) *cyclohexyl* ^{13}C {^{1}H NMR} (CD$_3$CN, 298 K): 155.3 *acetamidine-C$_a$*; 151.2 *pyrazole-C$_3$*; 142.0 *pyrazole-C$_5$*; 107.4 *pyrazole-C$_4$*; 68.5 *THF*; 62.4 *acetamidinate-C$_b$*; 55.2 *cyclohexyl-NCH$_\beta$*; 54.4 *cyclohexyl-NCH$_\alpha$*; 35.3 *cyclohexyl*; 33.8 *cyclohexyl*; 26.4–25.2 *cyclohexyl + THF*; 13.3 *pyrazole-Me$_3$*; 11.3 *pyrazole-Me$_5$*
4	^{1}H NMR (CD$_3$CN, 298 K): 6.86 (s, 1H) *acetamidinate-H$_b$*; 5.94 (s, 2H) *pyrazole-H$_4$*; 3.68 (m, br, 4H) *THF*; 3.41 (m, 1H) *cyclohexyl-NCH$_\alpha$*; 3.18 (m, 1H) *cyclohexyl-NCH$_\beta$*; 2.40 (s, 6H) *pyrazole-Me$_5$*; 2.20 (s, 6H) *pyrazole-Me$_3$*; 1.81 (m, 4H) *THF*; 1.78–1.01 (m, 20H) *cyclohexyl* ^{13}C {^{1}H NMR} (CD$_3$CN, 298 K): 152.2 *acetamidinate-C$_a$*; 151.2 *pyrazole-C$_3$*; 141.9 *pyrazole-C$_5$*; 107.4 *pyrazole-C$_4$*; 68.4 *THF*; 62.5 *acetamidinate-C$_b$*; 54.3 *cyclohexyl-NCH$_\beta$*; 53.8 *cyclohexyl-NCH$_\alpha$*; 35.3 *cyclohexyl*; 33.8 *cyclohexyl*; 26.2 *cyclohexyl*; 26.1 *cyclohexyl*; 25.8 *cyclohexyl*; 25.7 *cyclohexyl*; 25.5 *THF*; 13.3 *pyrazole-Me$_3$*; 11.3 *pyrazole-Me$_5$* Mass data (E.I., 70 eV, *m/z*): 810 [M$^{\bullet+}$–THF–F–F]$^+$; 679 [M$^{\bullet+}$–THF–SO$_3$CF$_3$–F]$^{\bullet+}$; 564 [M$^{\bullet+}$–THF–SO$_3$CF$_3$–SO$_2$CF$_3$]$^{\bullet+}$
5	Mass data (E.I., 70 eV, *m/z*): 686 [M$^{\bullet+}$–THF–SO$_3$CF$_3$–F]$^{\bullet+}$; 571 [M$^{\bullet+}$–THF–SO$_3$CF$_3$–SO$_2$CF$_3$]$^{\bullet+}$
6	Mass data (E.I., 70 eV, *m/z*): 823 [M$^{\bullet+}$–THF–F–F]$^{\bullet+}$; 577 [M$^{\bullet+}$–THF–SO$_3$CF$_3$–SO$_2$CF$_3$]$^{\bullet+}$; 561 [M$^{\bullet+}$–THF–SO$_3$CF$_3$–SO$_3$CF$_3$]$^{\bullet+}$
7	Mass data (E.I., 70 eV, *m/z*): 702 [M$^{\bullet+}$–THF–SO$_3$CF$_3$–F]$^{\bullet+}$; 588 [M$^{\bullet+}$–THF–SO$_3$CF$_3$–SO$_2$CF$_3$]$^{\bullet+}$
8	Mass data (E.I., 70 eV, *m/z*): 730 [M$^{\bullet+}$–THF–SO$_2$CF$_3$–F]$^+$; 599 [M$^{\bullet+}$–THF–SO$_3$CF$_3$–SO$_2$CF$_3$]$^{\bullet+}$

Pyrazole-C$_4$ signal falls around 107–109 ppm, while acetamidinate-C$_b$ shows a resonance between 66 and 62 ppm. The cyclohexyl N-bonded carbon atoms fall in the range 57–51 ppm, while the other cyclohexyl ^{13}C NMR resonances are comprised between 36 and 23 ppm. The most upfield signals correspond to the pyrazole methyl substituents. The ^{13}C{^{1}H} NMR spectra of **2**–**4** confirm the presence of a THF molecule. The described ^{1}H and ^{13}C{^{1}H} NMR spectra show a simple set of resonances for the pyrazole rings, indicating that both the groups are equivalent. These data suggest an octahedral disposition for the metal atoms with κ^3-NNN-coordination of the heteroscorpionate ligand, a situation where a plane of symmetry exists and contains the amidinate group and the metal center. The NMR signals due to the amidinate moiety show two sets of resonances for the NCH protons in the ^{1}H NMR spectra and eight cyclohexyl resonances in the ^{13}C{^{1}H} NMR spectra. This observation is indicative of a monodentate binding of the amidinate group to the metal center, which has already observed for complexes of elements of groups 1, 2, 4 and 12 [6,17], as depicted in Scheme 1. Despite all the attempts we have been unable to isolate suitable crystals for the X-ray analyses.

The proposed geometry was confirmed by computational studies on the [Ln(OTf)$_2$(cybpamd)(THF)] derivatives {Ln = Sc (**2**), Y (**3**), La (**4**), Nd (**5**), Sm (**6**), Dy (**7**), Yb (**8**)}, whose structures were initially optimized with the PM6 Hamiltonian. The obtained ground-state geometries confirmed that cybpamd acts as a tridentate ligand with only one amidinate nitrogen atom strongly bonded to the lanthanum center. The singlet-state complexes of Sc, Y, and La **2**–**4** have been subsequently optimized by DFT EDF1/LACVP* calculations. As for the semi-empirical calculations, also the DFT results indicated that the scorpionate ligand is quite strongly bonded to the metal ions with three nitrogen atoms. The coordination mode of the two triflate groups is κ^1 and the sixth position of the octahedric coordination sphere is occupied by a THF molecule. The DFT-computed bond lengths for the complexes **2**–**4** are reported in Table 2, while their optimized geometries are depicted in Fig. 1.

The paramagnetic complexes **5**–**8** have been characterized by means of elemental analyses and mass spectrometry by comparing the theoretical and experimental isotopic patterns. The mass spectrum of the completely NMR characterized lanthanum derivative **4** was collected for comparison. All the MS spectra show signals assignable to the molecular ions after the loss of the coordinated THF and a number of fragments from the triflate groups, in particular F, SO$_2$CF$_3$ and SO$_3$CF$_3$, in agreement with the proposed formulations.

3.2. Polymerizations

Cationic alkyl complex of group 4 metals are the most common single-site olefin polymerization catalysts [18]. Isoelectronic neutral alkyl complexes of group 3 metals, due to lower electrophilicity, generally show much lower polymerization activity [3]. One possible approach to improve the catalytic performances involves the generation of cationic alkyl species by a suitable activator, therefore all synthesized compounds (**2**–**8**) were tested in the polymerization of ethylene after activation by methylaluminoxane (MAO). Moreover, triflate anions must be necessary removed from the coordination sphere of the rare-earths metal complexes. In order to give polymerization of ethylene the catalyst must have, over the ancillary ligands, a vacant site where it coordinates the monomer and an alkyl group where the insertion can take place. It is commonly accepted that the role of MAO consists in the alkylation and

Table 2
Computed EDF1/LACVP* metal–ligands bond lengths for the complexes **2**–**4**.

	Bond length (Å)		Bond length, Å
[Sc(OTf)$_2$(cybpamd)(THF)]			
Sc-N(pyrazole1)	2.380	Sc-O(triflate1)	2.043
Sc-N(pyrazole2)	2.366	Sc-O(triflate2)	2.044
Sc-N(acetamidine)	2.084	Sc-O(THF)	2.335
[Y(OTf)$_2$(cybpamd)(THF)]			
Y-N(pyrazole1)	2.518	Y-O(triflate1)	2.210
Y-N(pyrazole2)	2.532	Y-O(triflate2)	2.210
Y-N(acetamidine)	2.250	Y-O(THF)	2.473
[La(OTf)$_2$(cybpamd)(THF)]			
Y-N(pyrazole1)	2.704	Y-O(triflate1)	2.385
Y-N(pyrazole2)	2.712	Y-O(triflate2)	2.390
Y-N(acetamidine)	2.413	Y-O(THF)	2.681
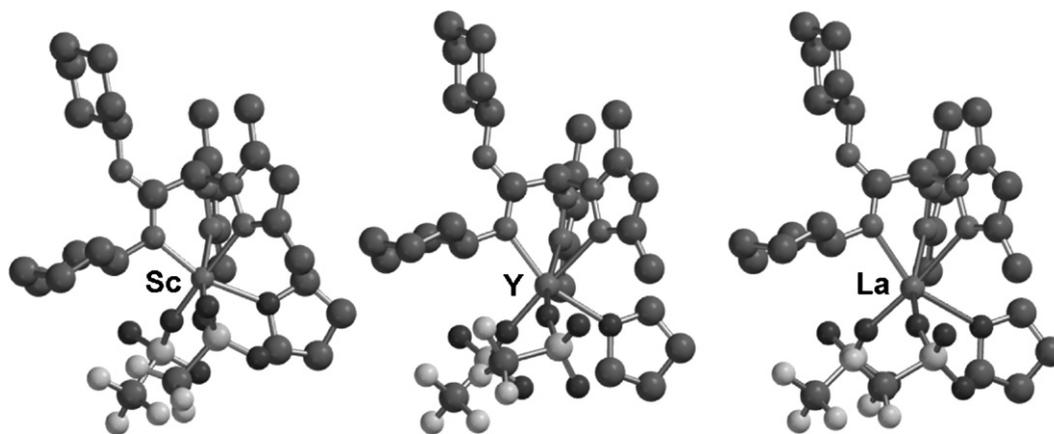
Fig. 1. DFT-optimized geometries of [Ln(OTf)$_2$(cybpamd)(THF)] {Ln = Sc (**2**), Y (**3**), La (**4**)}. Hydrogen atoms were omitted for clarity.

cationization of the catalytic precursor, producing the suitable catalytic site. We have recently reported as the role of MAO is essential to have group 3 complexes with fair activity [5b] and in the literature are reported a number of cationic alkyl complexes of the rare-earth metals able to polymerize ethylene [3].

Data reported in the Table 3 show that all the complexes **2–8** are able to polymerize ethylene, producing linear polyethylenes having a melting point higher than 135 °C and a high molecular weight (>6 × 10^5 Da). Moreover, the molecular weight distribution is in all the cases close to 2, revealing that the polymer are generate on single-site catalysts.

The most active catalysts in ethylene polymerization were those based on lanthanum (**4**), neodymium (**5**) and scandium (**2**) compounds. Complexes **2** and **4** were therefore tested also in the polymerization of propylene (see experimental part). Polypropylene having a substantially isotactic microstructure (*mm* triads concentration = 81%) was produced by the lanthanum derivative **4**, although with very low activity. Complex **2** was instead practically inactive. Probably, the high steric hindrance of the [N,N,N-scorpionate ligand] prevents the coordination of propene to the catalytic site.

The activities of the catalysts in the ethylene polymerization have been correlated to the ionic radii *r* of the metals [19,20] and the series Yb–Y–Dy–Sm–Nd–La follows the linear relationship (1), depicted in Fig. 2. The scandium-based catalyst gives instead a higher activity than that expectable on the bases of this activity–radius relationship.

$$\text{activity} = mr + q \quad \{\text{activity} = g_{polymer}/(\text{mol}_{cat}\,[\text{ethylene}]\,h); \, r = \text{Å}\,\} \tag{1}$$

m = 63,000 ± 4000 g$_{polymer}$/(mol$_{cat}$ [ethylene] h Å);
q = −61,000 ± 4000 g$_{polymer}$/(mol$_{cat}$ [ethylene] h).

Fig. 2. plot of the activity in ethylene polymerization of complexes **2–8** against Ln^{3+} ionic radius.

These findings can be rationalized by considering that the polymerization of ethylene was reported to occur as sequence of the following events: (i) coordination of monomeric unit to the metal bearing the ancillary ligand and the growing chain (ii) insertion of the activated monomer into the growing chain [21]. DFT EDF1/LACVP* calculations have been carried out on models for the active species of the type [Ln(CH$_3$)(CH$_2$=CH$_2$)(cybpamd)]$^+$ {Ln = Sc, Y, La} and a selection of computed data is reported in Table 4. The DFT-optimized geometries are reported in Fig. 3.

In all the three models the ancillary ligand cybpamd results bonded to the metal center with three nitrogen atoms. The ethylene molecule appears weakly coordinated, being the Ln–olefin bond

Table 3
Polymerizations of ethylene in the presence of complexes **2–8**.

Run[a]	Precatalyst	Ionic radius[b] (Å)	Yield (g)	Activity[c]	M_W[d] (×10^5)	M_W/M_n[d]
2	Sc	0.89	1.43	9669	7.3	2.2
3	Y	1.04	0.62	4192	7.7	2.0
4	La	1.17	1.93	13052	6.3	1.7
5	Sm	1.10	1.14	7708	8.8	1.9
6	Nd	1.12	1.47	9939	6.9	1.9
7	Dy	1.05	0.85	5747	9.1	2.2
8	Yb	1.01	0.45	3043	7.5	2.3

[a] Polymerization conditions: solvent toluene = 150 ml; precatalyst = 1.0 × 10^{-5}; cocatalyst: MAO (based on Al) = 8.6 × 10^{-3} mol; ethylene concentration in the feed = 0.87 M; temperature = 50 °C; time = 17 h.

[b] Ionic radii determined by the method of Shannon and Prewitt [19] and referred to Ln^{3+} hexacoordinated ions, taken from Ref. [20].

[c] Activity = g$_{polymer}$/(mol$_{cat}$ [ethylene] h).

[d] Weight and polydispersity index (M_W/M_n) determined by gel permeation chromatography versus polystyrene standard.

Fig. 3. DFT-optimized geometries of the [Ln(CH$_3$)(CH$_2$=CH$_2$)(cybpamd)]$^+$ {Ln = Sc, Y, La} active species models. Hydrogen atoms were omitted for clarity.

Table 4
Computed EDF1/LACVP* metal–ligands bond lengths and CH$_3$ Mulliken charge for the [Ln(CH$_3$)(CH$_2$=CH$_2$)(cybpamd)]$^+$ {Ln = Sc, Y, La} active species models.

	Bond length (Å)	CH$_3$ Mulliken charge
[Sc(CH$_3$)(CH$_2$=CH$_2$)(cybpamd)]$^+$		
Sc-N(pyrazole1)	2.251	−0.318
Sc-N(pyrazole2)	2.241	
Sc-N(acetamidine)	2.020	
Sc-ethylene	3.234	
Sc-CH$_3$	2.181	
[Y(CH$_3$)(CH$_2$=CH$_2$)(cybpamd)]$^+$		
Y-N(pyrazole1)	2.457	−0.304
Y-N(pyrazole2)	2.414	
Y-N(acetamidine)	2.184	
Y-ethylene	3.094	
Y-CH$_3$	2.355	
[La(CH$_3$)(CH$_2$=CH$_2$)(cybpamd)]$^+$		
La-N(pyrazole1)	2.673	−0.319
La-N(pyrazole2)	2.601	
La-N(acetamidine)	2.356	
La-ethylene	3.337	
La-CH$_3$	2.522	

length always greater than 3 Å. The Ln–CH$_3$ bond length is linearly related with the Ln^{3+} ionic radius, as depicted in Fig. 4.

The great Ln–ethylene bond lengths make the olefin poorly affected by the nature of the metal center. The first step of the polymerization reaction, i.e. the coordination of the monomeric unit to the metal, should therefore be scarcely dependent upon the ionic radius. The second event of the polymerization reaction, i.e. the insertion of the monomer into the growing chain, depends besides all upon the strength of the Ln–alkyl bond. The linear growth of the Ln–CH$_3$ on increasing the ionic radius reported in Fig. 4 can therefore explain the linear trend of Fig. 2, i.e. the activity growth along the series Yb–Y–Dy–Sm–Nd–La. To a greater ionic radius corresponds in fact a longer Ln–CH$_3$ bond and the alkyl migration on the coordinated olefin should therefore be favored for the greatest Ln(III) ions.
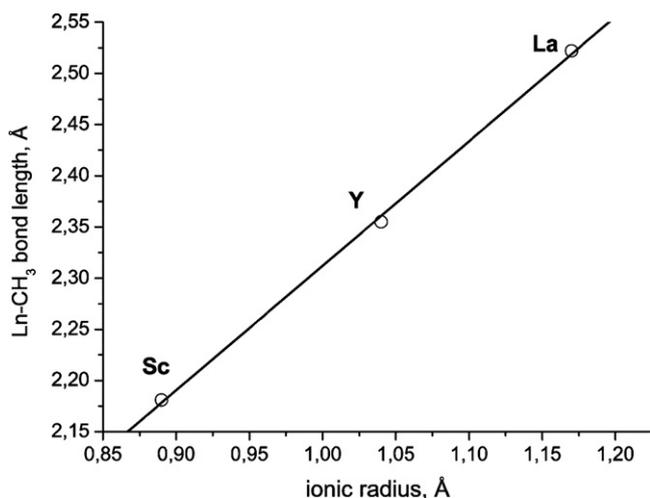
For the Sc-based catalytic system we have observed an activity value that is not correlated to the ionic radius, as observable in Fig. 2. It can be tentatively proposed that the really high hardness of Sc^{3+} with respect to those of the Ln^{3+} ions could cause a greater activation of the coordinated alkyl group, thus the [Ln]–CH$_3$ Mulliken charges were computed to support such an hypothesis. The CH$_3$ change varies from −0.304 to −0.319 on changing the metal ion from Y lo La, but this is an expectable behavior associated to the increase of the bond length and the growth of the Ln–C ionic character. In the [Sc(CH$_3$)(CH$_2$=CH$_2$)(cybpamd)]$^+$ model the coordinated alkyl charge is instead not related with the Sc–C bond length. Despite this bond is short (2.181 Å), the –CH$_3$ group has in fact a negative partial charge of −0.318, which is comparable to that of the lanthanum derivative (−0.319). This means that scandium(III) polarizes the bond with the alkyl group more than the expected only on the basis of the ionic radius, making therefore faster the olefin insertion. The particular electronic features of Sc(III) with respect to the other metal centers studied in this work are the causes of the different catalytic activity observed towards ethylene polymerization.

4. Conclusions

In this paper the synthesis and characterization of a series of new group 3 and lanthanide [N,N,N]-heteroscorpionate triflate-complexes has been reported and the coordination geometry has been suggested both on the basis of the analytical, spectroscopic, MS data and by optimized structural calculations. Catalytic tests towards ethylene polymerization highlighted the correlation between the properties of the metal center and the catalytic activity of the corresponding complexes. DFT calculations on active species models allowed proposing an explanation for the observed catalytic activities.

The very low activities showed in the polymerization of propylene by the catalytic systems based on compounds **4** and **2** could probably be improved using precatalysts having ancillary ligands with lower steric hindrance. Work is currently in progress in order to verify this hypothesis.

Fig. 4. Relationship between metal center ionic radius and Ln–CH$_3$ bond length in [Ln(CH$_3$)(CH$_2$=CH$_2$)(cybpamd)]$^+$ active species models.

Acknowledgments

References

[1] (a) K.W. Bagnall, A.C. Tempest, J. Takats, A.P. Masino, Inorg. Nucl. Chem. Lett. 12 (1976) 555;
(b) M.V.R. Stainer, J. Takats, Inorg. Chem. 21 (1982) 4050.

[2] (a) S. Trofimenko, The Coordination Chemistry of Polypyrazolylborate Ligands, Imperial College Press, London, 1999;
(b) C. Pettinari, C. Santini, in: J.A. McCleverty, T.J. Meyer (Eds.), Comprehensive Coordination Chemistry II, vol. 1, Elsevier, Oxford, 2004, pp. 159–210;
(c) S. Trofimenko, Chem. Rev. 93 (1993) 943;
(d) C. Pettinari, R. Pettinari, Coord. Chem. Rev. 249 (525) (2005) 663;
(e) N. Marques, A. Sella, J. Takats, Chem. Rev. 102 (2002);
(f) W.E. Piers, D.J.H. Emslie, Coord. Chem. Rev. 233 (2002) 131;
(g) I. Santos, N. Marques, N. J. Chem. 19 (1995) 551;
(h) F.D. Edelmann, Angew. Chem. Int. Ed. Engl. 40 (2001) 1656;
(i) A. Otero, J. Fernandez-Baeza, A. Antiñolo, J. Tejeda, A. Lara-Sanchez, L. Sanchez-Barba, E. Martinez-Caballero, A.M. Rodriguez, I. Lopez-Solera, Inorg. Chem. 44 (2005) 5336;
(j) P. Mountford, B.D. Ward, Chem. Commun. (2003) 1797;
(k) M. Zimmermann, J. Takats, G. Kiel, K.W. Tornroos, R. Anwander, Chem. Commun. (2008) 612.

[3] For some references see:
(a) M.E. Thompson, J.E. Berkaw, Pure Appl. Chem. 56 (1984) 1;
(b) S. Arndt, K. Beckerle, P.M. Zeimentz, T.P. Spaniol, J. Okuda, Angew. Chem. Int. Ed. 44 (2005) 7473;
(c) C.S. Tredget, F. Bonnet, A.R. Cowley, P. Mountford, Chem. Commun. (2005) 3301;
(d) S. Arndt, T.P. Spaniol, J. Okuda, Angew. Chem. Int. Ed. 42 (2003) 5075;
(e) P.M. Zeimentz, S. Arndt, B.R. Elvidge, J. Okuda, Chem. Rev. 106 (2006) 2404;
(f) S. Arndt, J. Okuda, Chem. Rev. 102 (2002) 1953.

[4] (a) S.C. Lawrence, B.D. Ward, S.R. Dubberley, C.M. Kozak, P. Mountford, Chem. Commun. (2003) 2880;
(b) D.P. Long, P.A. Bianconi, J. Am. Chem. Soc. 118 (1996) 12453;
(c) B.D. Ward, S. Bellemin-Laponnaz, L.H. Gade, Angew. Chem. Int. Ed. 44 (2005) 1668.

[5] (a) G. Paolucci, A. Zanella, M. Bortoluzzi, S. Sostero, P. Longo, M. Napoli, J. Mol. Catal. A: Chem. 272 (2007) 258;
(b) G. Paolucci, M. Bortoluzzi, M. Napoli, P. Longo, J. Mol. Catal. A: Chem. 287 (2008) 121;
(c) G. Paolucci, M. Bortoluzzi, V. Bertolasi, Eur. J. Inorg. Chem. (2008) 4126;
(d) G. Paolucci, M. Bortoluzzi, S. Milione, A. Grassi, Inorg. Chim. Acta (2009), doi:10.1016/j.ica.2009.01.020.

[6] (a) L.F. Sánchez-Barba, A. Garcés, M. Fajardo, C. Alonso-Moreno, J. Fernández-Baeza, A. Otero, A. Antiñolo, J. Tejeda, A. Lara-Sánchez, M.I. López-Solera, Organometallics 26 (2007) 6403;
(b) C. Alonso-Moreno, A. Garcés, L.F. Sánchez-Barba, M. Fajardo, J. Fernández-Baeza, A. Otero, A. Lara-Sánchez, A. Antiñolo, L. Broomfield, M.I. López-Solera, A.M. Rodríguez, Organometallics 27 (2008) 1310.

[7] S. Kobayashi, M. Sugiura, H. Kitagawa, W.W.-L. Lam, Chem. Rev. 102 (2002) 2227.

[8] D.L. Jameson, R.K. Castellano, Inorg. Synth. 32 (1998) 58.

[9] (a) G. Balacco, J. Chem. Inf. Comput. Sci. 34 (1994) 1235;
(b) J.C. Cobas Gómez, F.J. Sardina López, MestRe-C, Universidad de Santiago de Compostela, Spain, 2006.

[10] J.J.P. Stewart, MOPAC2007, Version 7.295W, Stewart Computational Chemistry; http://openmopac.net.

[11] J.J.P. Stewart, J. Mol. Mod. 13 (2007) 1173.

[12] (a) R.O. Freire, N.B. da Costa Jr., G.B. Rocha, A.M. Simas, J. Chem. Theory Comput. 3 (2007) 1588;
(b) R.O. Freire, G.B. Rocha, A.M. Simas, Chem. Phys. Lett. 441 (2007) 354;
(c) N.B. da Costa Jr., R.O. Freire, G.B. Rocha, A.M. Simas, Inorg. Chem. Commun. 8 (2005) 831.

[13] R.D. Adamson, P.M.W. Gill, J.A. Pople, Chem. Phys. Lett. 284 (1998) 6.

[14] (a) P.J. Hay, R.W. Wadt, J. Chem. Phys. 82 (1985) 270;
(b) P.J. Hay, R.W. Wadt, J. Chem. Phys. 82 (1985) 299;
(c) M. Dolg, in: J. Grotendorst (Ed.), Modern Methods and Algorithms of Quantum Chemistry, NIC Series, vol. 1, John von Neumann Institute for Computing, Jülich, 2000, pp. 479–508.

[15] (a) R.S. Mulliken, J. Chem. Phys. 23 (1955) 1833;
(b) R.S. Mulliken, J. Chem. Phys. 23 (1955) 1841;
(c) R.S. Mulliken, J. Chem. Phys. 23 (23) (1955) 2338;
(d) R.S. Mulliken, J. Chem. Phys. 23 (1955) 2343.

[16] Spartan '08, version 1.1.1, B.J. Deppmeier, A.J. Driessen, T.S. Hehre, W.J. Hahre, J.A. Johnson, P.E. Klunzinger, J.M. Leonard, I.N. Pham, W.J. Pietro, J. Yu, Y. Shao, L. Fusti-Molnar, Y. Jung, J. Kussmann, C. Ochsenfeld, S.T. Brown, A.T.B. Gilbert, L.V. Slipchenko, S.V. Levchenko, D.P. O'Neill, R.A. DiStasio Jr., R.C. Lochan, T. Wang, G.J.O. Beran, N.A. Besley, J.M., Herbert, C.Y. Lin, T. Van Voorhis, S.H. Chien, A. Sodt, R.P. Steele, V.A. Rassolov, P.E. Maslen, P.P. Korambath, R.D. Adamson, B. Austin, J. Baker, E.F.C. Byrd, H. Dachsel, R.J. Doerksen, A. Dreuw, B.D. Dunietz, A.D. Dutoi, T.R. Furlani, S.R. Gwaltney, A. Heyden, S. Hirata, C.-P. Hsu, G. Kedziora, R.Z. Khalliulin, P. Klunzinger, A.M. Lee, M.S. Lee, W. Liang, I. Lotan, N. Nair, B. Peters, E.I. Proynov, P.A. Pieniazek, Y.M. Rhee, J. Ritchie, E. Rosta, C. D. Sherrill, A.C. Simmonett, J.E. Subotnik, H.L. Woodcock III, W. Zhang, A.T. Bell, A.K. Chakraborty, D.M. Chipman, F.J. Keil, A. Warshel, W.J. Hehre, H.F. Schaefer III, J. Kong, A.I. Krylov, P.M.W. Gill, M. Head-Gordon, Wavefun Inc., Irvine, CA.

[17] A. Otero, J. Fernández-Baeza, A. Antiñolo, J. Tejeda, A. Lara-Sánchez, L.F. Sánchez-Barba, I. López-Solera, A.M. Rodríguez, Inorg. Chem. 46 (2007) 1760.

[18] For some references see:
(a) W. Kaminsky, K. Kulper, H.H. Brintzinger, F. Wild, Angew. Chem. Int. Ed. Engl. 24 (1985) 507;
(b) H.H. Brintzinger, D. Fischer, R. Mullhaupt, D. Rieger, R.M. Waymouth, Angew. Chem. Int. Ed. Engl. 34 (1995) 1143;
(c) L. Resconi, L. Cavallo, A. Fait, F. Piemontesi, Chem. Rev. 100 (2000) 1253;
(d) J.A. Ewen, J. Am. Chem. Soc. 106 (1984) 6355;
(e) J.A. Ewen, R.L. Jones, A. Razavi, J. Ferrara, J. Am. Chem. Soc. 110 (1988) 6255;
(f) G.G. Hlarky, H.W. Turner, R.R. Eckman, J. Am. Chem. Soc. 111 (1989) 2728;
(g) C. Pellecchia, A. Proto, P. Longo, A. Zambelli, Makromol. Chem. Rapid Commun. 12 (1991) 663;
(h) C. Pellecchia, A. Proto, P. Longo, A. Zambelli, Makromol. Chem. Rapid Commun. 13 (1992) 277;
(i) T. Fujita, Y. Tohi, M. Mitani, S. Matsui, J. Saito, M. Nitabaru, K. Sugi, H. Makio, T. Tsutsui, European Patent, EP 0874005 (1998), to Mitsui Chemicals Inc;
(j) S. Matsui, Y. Tohi, M. Mitani, J. Saito, H. Makio, Y. Matsukawa, S. Matsui, J.I. Mohri, R. Furuyama, Y. Terao, H. Bando, H. Tanaka, T. Fujita, Chem. Lett. (1999) 1065;
(k) M. Mitani, J. Saito, S.I. Ishii, Y. Nakayama, H. Makio, Y. Matsukawa, S. Matsui, J.I. Mohri, R. Furuyama, Y. Terao, H. Bando, H. Tanaka, T. Fujita, Chem. Rec. 4 (2004) 137;
(l) H. Makio, T. Fujita, Bull. Chem. Soc. Jpn. 78 (2005) 52;
(m) J. Saito, M. Mitani, J. Mohri, Y. Yoshida, S. Matsui, S. Ishii, S. Kojoh, N. Kashiwa, T. Fujita, Angew. Chem. Int. Ed. 40 (2001) 2918;
(n) M. Mitani, J. Mohri, Y. Yoshida, J. Saito, S. Ishii, K. Tsuru, S. Matsui, R. Furuyama, T. Nakano, H. Tanaka, S. Kojoh, T. Matsugi, N. Ashiwa, T. Fujita, J. Am. Chem. Soc. 124 (2002) 3327.

[19] (a) R.D. Shannon, C.T. Prewitt, Acta Crystallogr. B 25 (1969) 925;
(b) R.D. Shannon, Acta Crystallogr. A 32 (1976) 751.

[20] F.A. Cotton, G. Wilkinson, A.C. Murillo, M. Bochmann, Advanced Inorganic Chemistry, 6th edition, John Wiley and Sons, New York, 1999.

[21] E.J. Arlman, P. Cossee, J. Catal. 3 (1964) 89.